

X_{1c} -like levels in superlattices, as one applies pressure,^{9(a)} electric,^{9(b)} or magnetic^{9(c)} fields. This nonzero coupling can be described via atomistic theories such as tightbinding¹⁰ or pseudopotentials,¹¹ but vanishes in the standard model EFA:

$$V_{\Gamma,X}^{EFA} = 0. \quad (1)$$

Pseudopotential calculations¹¹ quantitatively predicted this coupling potential vs the superlattice period n , showing that it vanishes for $n = \text{odd}$, and obtaining the effects of pressure in good agreement with experiment.

(ii) *The light-hole to heavy-hole coupling $V_{lh,hh}$ in (001) superlattices*, which leads at $\mathbf{k}_{\parallel} = 0$ to the observed^{12,13} anticrossing of lh_1 with hh_2 excitons. In the D_{2d} point group symmetry of a (001) superlattice having a *common atom* (such as AlAs/GaAs), or in the C_{2v} symmetry of *non-common-atom* (001) superlattices such as InAs/GaSb, the lh_1 and hh_2 states have the same Γ_7 symmetry representation, so they must anticross rather than cross. Atomistic theories such as tightbinding¹⁴ and pseudopotential^{15,16} for the D_{2d} superlattices, and pseudopotential⁸ theory for the C_{2v} superlattices, indeed produce^{8,14-16} anticrossing at $\mathbf{k}_{\parallel} = 0$ [see Fig. 3(b) in Ref. 8]. On the other hand, the standard EFA, being a continuum theory, lacks this anticrossing at $\mathbf{k}_{\parallel} = 0$, since it assumes

$$V_{lh,hh}^{EFA}(\mathbf{k}_{\parallel} = 0) = 0 \quad (2a)$$

and

$$V_{lh,hh}^{EFA}(\mathbf{k}_{\parallel} \neq 0) \neq 0. \quad (2b)$$

The effects of the $V_{lh,hh}(\mathbf{k}_{\parallel} = 0)$ coupling are amplified enormously in C_{2v} non-common-atom superlattices such as GaInAs/InP (001) or InAs/GaSb (001) and reveal themselves through a giant in-plane polarization anisotropy in the optical absorption,¹⁷ which is not present in D_{2d} superlattices. While atomistic models *force* lh-hh mixing at $\mathbf{k}_{\parallel} = 0$ upon us by the very nature of the symmetry properties of the relevant states, such mixing can only be *accommodated* in the standard model of EFA if additional terms are added ‘‘by hand’’ to the boundary conditions at the interface¹⁸ or to the EFA Hamiltonian.¹⁷ The theory itself does not provide the magnitude of $V_{lh,hh}(\mathbf{k}_{\parallel} = 0)$, which thus needs to be supplied externally.

(iii) *The electron-heavy-hole coupling $V_{e,hh}$ in non-common-atom superlattices* that leads (a) at $\mathbf{k}_{\parallel} = 0$, to a small anticrossing gap at $n = n_c$ ⁸ as well as to an in-plane polarization anisotropy in the optical absorption⁸ and (b) at $\mathbf{k}_{\parallel} \neq 0$ to the ‘‘hybridization gap’’ for $n > n_c$.⁵ Again, atomistic theories predict the $\mathbf{k}_{\parallel} = 0$ anticrossing gap and the $\mathbf{k}_{\parallel} = 0$ polarization anisotropy.^{8,19} The standard model of EFA, however, results in

$$V_{e,hh}^{EFA}(\mathbf{k}_{\parallel} = 0) = 0 \quad (3a)$$

and

$$V_{e,hh}^{EFA}(\mathbf{k}_{\parallel} \neq 0) \neq 0. \quad (3b)$$

So while EFA-based methods can explain at least qualitatively the in-plane $\mathbf{k}_{\parallel} \neq 0$ hybridization gap underlying Eq. (3b), they cannot account for the anticrossing behavior at $\mathbf{k}_{\parallel} = 0$ for $n = n_c$ (electron and hole states cross in EFA rather

than anticross) nor the $\mathbf{k}_{\parallel} = 0$ polarization anisotropy. Note that Eq. (3a) is a consequence of the fact that $V_{lh,hh}^{EFA}(\mathbf{k}_{\parallel} = 0) = 0$. Again, it is possible to add by hand additional terms to EFA to introduce the missing band couplings.²⁰ However, the value of the coupling constant is undetermined by that theory.

III. CALCULATION OF THE HYBRIDIZATION GAP

We see from the forgoing discussion that the problem of predicting the hybridization gap in non-common-atom superlattices is relatively easy, because already the standard model grants a nonzero coupling in Eq. (3b). This should be contrasted with the more difficult problems of predicting the $\mathbf{k}_{\parallel} = 0$ lh-hh coupling [Eq. (2a)] or the $\Gamma - X$ coupling [Eq. (1)], where, by itself, the standard model provides a null effect. However, the problem of determining the hybridization gap is not entirely trivial, because it is not obvious whether EFA gives the right *magnitude* of the gap. There are two reasons to raise this question: (1) The absence of $V_{e,hh}^{EFA}(\mathbf{k}_{\parallel} = 0)$ can affect the $V_{e,hh}(\mathbf{k}_{\parallel} \neq 0)$ coupling and thus the hybridization gap at $\mathbf{k}_{\parallel} \neq 0$; (2) the e -hh coupling comes from the interaction between the InAs-localized electron state and the GaSb-localized heavy-hole state. The magnitude of these couplings sensitively depends on the detailed boundary conditions used at the interface, which are an unsettled issue in the EFA theory.^{18,21,22}

While EFA-based models of band coupling involve complex discussions of various boundary condition choices (e.g., see Refs. 6, 18, 21, and references therein), atomistic models are free from such ambiguity, directly provide the magnitude of the coupling constants, and are simple to apply. Recent pseudopotential calculations on $(\text{InAs})_n/(\text{GaSb})_n$ (001) superlattices⁸ indeed demonstrated (1) the existence of in-plane polarization anisotropy of the e -hh transitions at $\mathbf{k}_{\parallel} = 0$; (2) the occurrence of e 1-hh1 mixing at $\mathbf{k}_{\parallel} = 0$ around $n = 28$; and (3) the anticrossing of the second and third hole states lh_1 and hh_2 at $\mathbf{k}_{\parallel} = 0$. Because of Eq. (3a) these properties could not be predicted by the standard $\mathbf{k} \cdot \mathbf{p}$ approach. Here we use the same pseudopotential model to study the $\mathbf{k}_{\parallel} \neq 0$ dispersion in $(\text{InAs})_n/(\text{GaSb})_m$ superlattices strained to the lattice constant of a GaSb substrate, thus determining the anticrossing gap.

In the pseudopotential theory (P theory) used here,⁸ the single-particle Schrödinger equation is given by

$$\left[-\frac{\beta}{2} \nabla^2 + \sum_{n\alpha} v_{\alpha}(r - R_{n\alpha}) \right] \psi_i(r) = \epsilon_i \psi_i(r), \quad (4)$$

where $R_{n\alpha}$ denotes the position of the n th atom of type α . The atomic positions are determined by minimizing the atomistic strain energy of the superlattice.⁸ This results in the InAs and GaSb segments having tetragonal c/a ratios close to one, whereas the two interfaces have a dilated InSb bond ($c/a = 1.13$) and a compressed GaAs bond ($c/a = 0.85$). The screened pseudopotentials $\{v_{\alpha}\}$ are determined⁸ by fitting to the measured *all-zone* (i.e., not just Γ) bulk band structures of InAs and GaSb (including anisotropic effective masses), and to the local-density approximation (LDA) calculated band offsets and deformation potentials. Spin-orbit interactions are included as a nonlocal part of v_{α} . The coefficient β

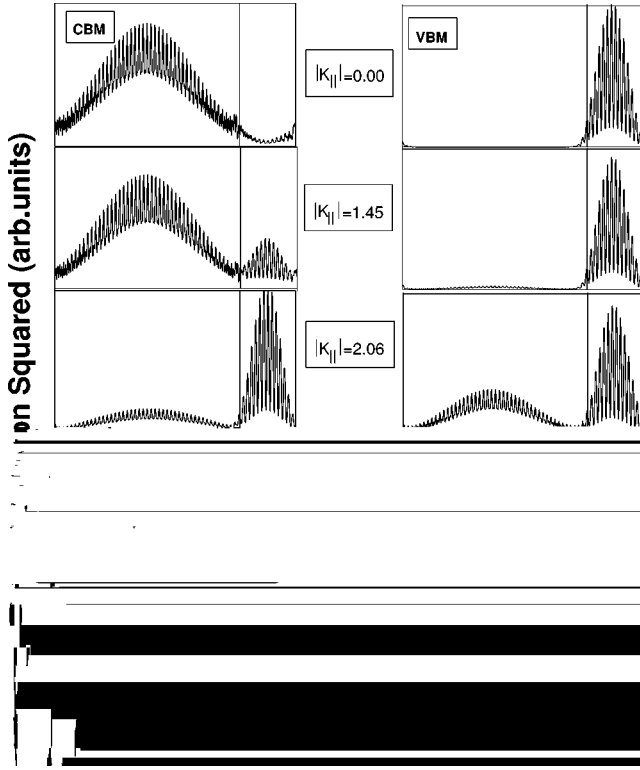


FIG. 3. Evolution of the wave function of the last occupied state (left column) and the first unoccupied state (right column) of the $(\text{InAs})_{46}(\text{GaSb})_{14}$ (001) superlattice along the in-plane $\mathbf{k}_{\parallel}=(k_x=k_y)$ direction at $k_z=0$. Wave functions are averaged over the in-plane coordinates.

thicknesses n and m are changed. We have considered a $(\text{InAs})_{30}/(\text{GaSb})_{30}$ superlattice with the same total $n+m$ period as the previously studied $(\text{InAs})_{46}/(\text{GaSb})_{14}$ superlattice. The pseudopotential calculated in-plane dispersion relations of the two superlattices along the $k_x=k_y$ direction at $k_z=0$ are compared in Fig. 4. Since the well widths determine the confinement energies, using the (30,30) period rather than (46,14) leads to a more confined electron (since the InAs electron well is now narrower) and to a less confined heavy hole (since the GaSb hole well is now wider). Thus, the (30,30) superlattice has a smaller (negative) gap at $\mathbf{k}_{\parallel}=0$ than the (46,14) superlattice. The negative gap at $\mathbf{k}_{\parallel}=0$ is now 17 meV, i.e., about one-fourth of the corresponding gap of the (46,14) superlattice. Since the electron and heavy-hole bands are already closer to each other at $\mathbf{k}_{\parallel}=0$ than in the (46,14) case, the anticrossing point \mathbf{k}_{\parallel}^* occurs

TABLE I. Pseudopotential (P) and $\mathbf{k}\cdot\mathbf{p}$ calculated hybridization (H) gaps for a $(\text{InAs})_{46}(\text{GaSb})_{14}$ (001) superlattice. The band offset between the strained InAs CBM and GaSb VBM is 190 meV. In parentheses we give the band gaps obtained with a 150-meV offset.

Method	$E(\mathbf{k}_{\parallel}=0)$ (meV)		$E_H(\mathbf{k}_{\parallel}=\mathbf{k}^*)$ (meV)	
	$k_z=0$	$k_z=\frac{\pi}{L_z}$	$k_z=0$	$k_z=\frac{\pi}{L_z}$
P theory	65	45	25	8
$\mathbf{k}\cdot\mathbf{p}$	68(32)	38(8)	29(22)	8(1.5)

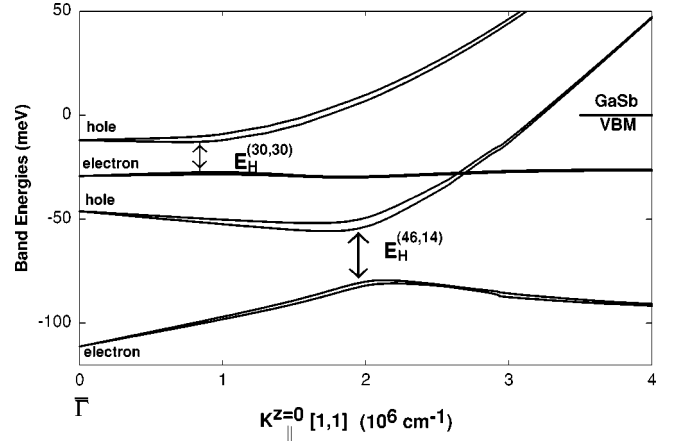


FIG. 4. Comparison between the pseudopotential calculated dispersion relations of a $(\text{InAs})_{46}(\text{GaSb})_{14}$ superlattice and of a $(\text{InAs})_{30}(\text{GaSb})_{30}$ along the $(k_x=k_y)$ direction at $k_z=0$.

closer to the Brillouin zone center. However, we see that the interaction V_{e-hh} in this region given by the pseudopotential theory is relatively strong, and, as a consequence, the hybridization gap is 15 meV wide, not much smaller than the negative gap at $\mathbf{k}_{\parallel}=0$.

We have also examined the interband transition dipole matrix elements for the (30,30) superlattice and found that, while the transitions at $\mathbf{k}_{\parallel}=0$ have the same intensity as those in the (46,14) superlattice, both the intensity and the polarization anisotropy of the transitions at \mathbf{k}_{\parallel}^* are smaller than those we have found in the (46,14) superlattice. Thus, we see that, the closer E_H is to $\mathbf{k}_{\parallel}=0$, the less intense and anisotropic are the interband transitions.

E. Comparison of pseudopotential and model calculations

Figure 5 compares the pseudopotential results with the model calculation of de-Leon *et al.*⁶ for the $(\text{InAs})_{46}(\text{GaSb})_{14}$ system. The model of Ref. 6 describes the system as an InAs electron well interacting with a GaSb hole well, both wells being sandwiched between infinite barriers. Although two coupled quantum wells are a very simplified model of the system we are studying here, it is instructive to compare qualitatively our calculation with this model. The two systems are different in that the $(\text{InAs})_{46}(\text{GaSb})_{14}$ superlattice is a periodic system, showing a dispersion of the electron and hole bands along the k_z direction while there is no k_z dependence in the model of Ref. 6. The existence of the dispersion along k_z in our calculation reveals a coupling with other bands. In Ref. 6 the only allowed coupling is limited to the two electron and hole ground states of the uncoupled wells.

In Fig. 5 we compare the in-plane dispersions of the model in Ref. 6 with the superlattice dispersion for $k_z=0$. We see that the values of \mathbf{k}_{\parallel}^* at the anticrossing points are similar in both calculations. We can think of our $k_z=0$ superlattice wave function as a periodic repetition of the corresponding quantum well wave function without any complication of additional phase factors. Now, however, in addition to the mixing due to the perturbation at the InAs/GaSb interface, which is present in the model of Ref. 6, we have an additional perturbation at the GaSb/InAs interface. As a re-

sult, the anticrossing gap at \mathbf{k}

